Supplementary Information for

Peptide-Metal Interactions: A Comparison Between Solution and the Gas Phase

Yana Berezovskaya, Craig T. Armstrong, Aimee L. Boyle, Massimiliano Porrini, Derek N. Woolfson and Perdita E. Barran

A. Materials

vCP1 was synthesised using a Liberty CEM microwave synthesiser using standard Fmoc chemistry, rink-amide resin and HBTU activation. vCP1 was *N*-terminally acetylated and *C*-terminally amidated. The peptide was purified by reversed-phase HPLC and the identity confirmed by MALDI-TOF mass spectrometry using α-cyano-4-hydroxycinnamic acid (CHCA) matrix.

The buffer conditions for the CD and UV specstroscopic measurments were: 5% isopropanol; 20 mM ammonium acetate; pH 7.2; 500 μM TCEP. These were adjusted slightly for MS experiments to: 5% isopropanol; 10 mM ammonium acetate; pH 6.8; 200 μM TCEP. For MS analysis the stock solution was diluted to 20 μM concentration using solvents and reagents purchased from Fisher Scientific: LC-MS grade water, analytical reagent grade isopropanol, laboratory reagent grade ammonium acetate.

B. CD and other spectroscopic data

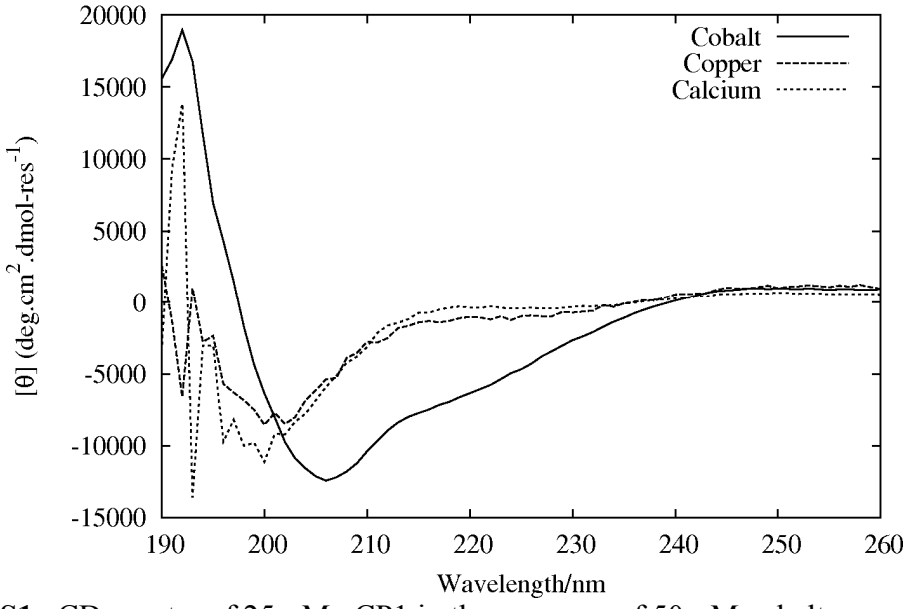

Figure S1. CD spectra of 25 μM vCP1 in the presence of 50 μM cobalt, copper and calcium. The cobalt spectrum is similar (although not identical) to that obtained using zinc. The copper and calcium spectra are more apo-like.

CD measurements were recorded using a JASCO-J815 spectropolarimeter fitted with a Peltier temperature controller. Peptide solutions were prepared at a concentration of 25 μM peptide in acetate buffer (20 mM, pH 7.2), with 5% isopropanol and 500 μM TCEP. The solutions were made up to a total volume of 400 μl using nitrogen-

saturated, deionised water. Spectra were recorded at 20 °C, using a 50 nm min^{-1} scanning speed, a 1 nm interval, 1 nm bandwidth, a 2 second response time and were averaged over 128 scans. Ellipticities (in mdeg) were baseline corrected and then converted to molar ellipticities (deg cm^2 $dmol.res^{-1}$) by normalizing for the concentration of peptide bonds and for the pathlength of the cell. Zinc chloride was added to give c.a. 2:1 metal:peptide, and a further small addition added to ensure the CD spectrum represented an end-point.

UV/VIS measurements were made using a PerkinElmer Lambda-25 spectrophotometer in conjunction with a 1 cm quartz cell. 1 ml of 25 µM peptide was prepared in the same manner as the CD samples, and filtered to remove any dust. 900 µl of the filtrate was added to the UV cell, and the peptide concentration re-determined by measuring the absorbance at 280 nm and assuming an extinction coefficient of 1490 $M^{-1}cm^{-1}$. In the case of the cobalt titration, cobalt chloride solutions of varying concentrations were added sequentially to the cuvette in 2 µl aliquots, using a 5 µl Hamilton syringe. Spectra were recorded between 850 nm and 190 nm. The absorbance at 640 nm was used as an indicator of the amount of cobalt bound, and the shape of the spectrum between 500 and 750 nm used as an indicator of the coordination environment of the cobalt ion.

Binding data was fit to the equation:

$$f(x) = \frac{(x + A + K) + \sqrt{(x + A + K)^2 - 4Ax}}{2}$$ ***Equation 1***

This accounts for depletion of free peptide (x) and ligand (A) under tight-binding conditions, to give the K_D (K). In practice both K and A were floated when fitting the two curves to account for the error in extinction coefficients due to the environment of the chromophore tyrosine.

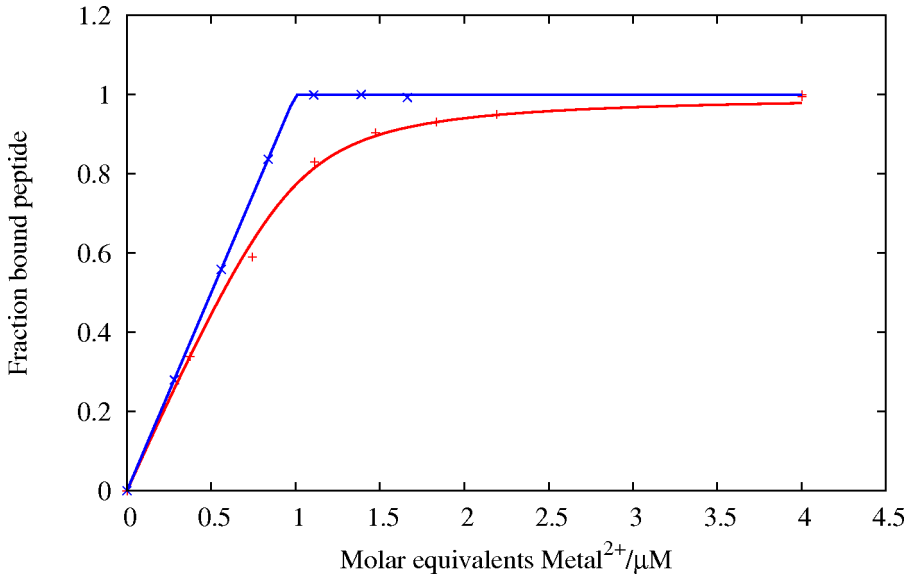

Figure S2. Fits to the binding data for the addition of zinc (blue) and cobalt (red) obtained from UV data. The K_D for Cobalt is estimated to be 0.8 μM and that for zinc is tight and sub-nanomolar.

C. Kd via Mass Spectrometry

The MS measurements were carried out on the Waters Q-ToF-2 instrument and analysed using the MassLynx v4.1 software. Nano-ESI conditions are summarised in the table below:

Source temperature	80 °C
Desolvation temperature	ambient
Capillary voltage	~1.40 kV
Cone voltage	30 V
ToF period	70 μs

To determine the equilibrium constants for the vCP1 binding Zn^{2+}, the peptide was incubated with increasing concentrations of ZnAc at pH 6.8, and the monoisotopic signal intensities for the apo and holo-vCP1 were summed for all charge states. An assumption has been made that (i) the total signal intensity for each individual species is proportional to the concentration of that species in the gas phase, and hence, in solution; (ii) the apo and holo-peptide yield the same signal response. Relative intensities of the MS signals have been recalculated into concentration units, the results of two experimental repeats have been averaged, and the ratio of molar concentration of bound Zn^{2+} to total molar concentration of the vCP1 was plotted against the concentration of the free ligand. A sigmoidal curve has been fitted to the data points, and the inflection point has given the value of the K_d = 13 μM.

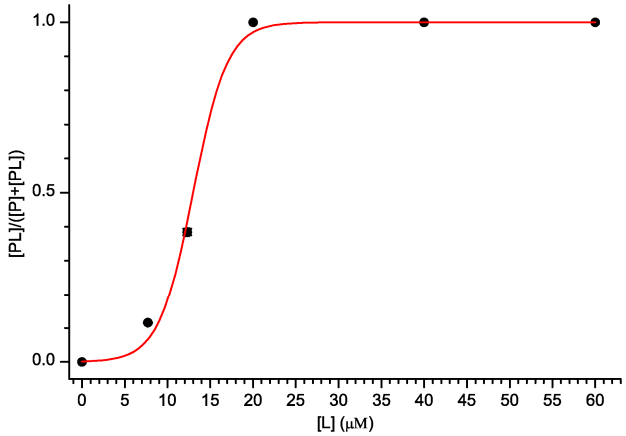

S3 the ratio of molar concentration of bound Zn^{2+} to total molar concentration of the vCP1 plotted against the concentration of free ligand. [P] – is the concentration of the free peptide, [L] – is the concentration of the free ligand, [PL] – is the concentration of bound ligand.

D. Ion-mobility mass spectrometry experimental details.

Ion mobility separates species based on their migration velocity in the presence of inert gas, commonly helium, in a linear electric field[1, 2]. An arrival time distribution (ATD) is measured during an ion mobility experiment. The mobility K of an ion is determined by the velocity v_d attained under the influence of a weak electric field E to traverse a drift cell of length L over time t_d:

$$\frac{L}{t_d} = v_d = KE \qquad \textit{Equation 1}$$

Ion mobility is normalised to standard pressure and temperature, yielding a reduced mobility K_0:

$$K_0 = K\frac{T_0}{T}\frac{P}{P_0} \qquad \textit{Equation 2}$$

Reduced mobility is determined experimentally, where z is the number of charges on the ion, N is the buffer gas number density at standard conditions, μ is the reduced mass of the analyte ion and buffer gas and Ω is the rotationally averaged collision cross-section:

$$K_0 = \frac{3ze}{16N}\left(\frac{2\pi}{\mu k_B T}\right)^{1/2}\frac{1}{\Omega} \qquad \textit{Equation 3}$$

Substituting the above equations, experimental collision cross-section Ω can be calculated, where k_B is the Boltzmann constant and e is the elementary charge:

$$\Omega = \frac{(18\pi)^{1/2}}{16N} \frac{ze}{(\mu k_B T)^{1/2}} \frac{t_d E}{L} \frac{760}{P} \frac{T}{273.2}$$ ***Equation 4***

Effectively the ions are separated based on their volume and shape. Thus, elongated ions would take longer to traverse through the drift tube than their compact structural isomers.

Ion-mobility mass spectrometry measurements were performed on the MoQToF, an in-house modified QToF 1 (Micromass UK Ltd.). It has been adapted to be capable of making temperature dependent collision cross section measurements, via the inclusion of a 5.1 cm long copper drift cell and supplementary ion optics situated post source optics and before the quadrupole analyser. This instrument and its operation has been described in detail elsewhere[3], but in brief ions are pulsed into the drift cell, where they drift through helium at a pressure of ~3.2-3.5 Torr, under the influence of a weak static electric field . On exiting the cell the ions then pass through a quadrupole mass analyser, which is run as a wide band pass filter, and then on to the time-of-flight mass spectrometer where they are detected via a stack of microchannel plates. Arrival time distributions are recorded for all of the ions detectable, and may be deconvoluted into selected ion arrival time distributions (ATDs) via Mass Lynx v4.1. The arrival time for each mass-selected ion is obtained from the experimentally measured time which equates to the time from ion injection into the cell until detection. This comprises the time taken for the ions to drift through the cell (drift time), plus the time the ions spent outside the drift cell (dead time). Since the second of these is fixed for a given m/z, measurements are made at several drift voltages (at least 6 over the range 60-15 V), to obtain the 'drift time' and the 'dead time'. The drift time of ions results from their mobility (K), which is inversely related to their rotationally averaged collision cross section (Ω). Here all measurements were taken at room temperature. A plot of experimentally measured arrival time versus P/V yields a slope whose gradient is 1/K, and whose intercept is the dead time. This is then converted to a reduced mobility K_0 and used to determine an experimental value for Ω via a modified version of the Mason-Schamp equation (see Equation 4)

E. Molecular Dynamics Simulations

The software package used for all the simulations was Amber10[4] and the force field implemented was Amber99, which does contain the divalent zinc atom parameters. The N-terminal proline and C-terminal glycine residues were protected with the acetyl (ACE) and N-methylamine (NME) groups, respectively, as for the synthetic peptide.

The three collision cross section time series were calculated using the MOBCAL code, which was developed by Prof. M. F. Jarrold. MOBCAL implements three different types of calculation to derive the collision cross section values between a polyatomic ion and helium (buffer gas):[5]

1. Projection approximation (PA), accurate only for small polyatomic ions (<1500 Da) with totally convex surfaces, ignore multiple scattering.
2. Exact hard spheres (EHS), takes into account multiple scattering
3. Trajectory method (TM), here the scattering angle is calculated via a more realistic potential, and the long range interaction is better described.

holo-vCP1

A homology model of the peptide based on the consensus zinc finger structure was submitted to the web site H++,[6] which automates the procedure of protonating the side chains of the residues, in according to the specified value of the solvent pH. The pH value was set to 7, to obtain a system total charge of +3.0. The model adopted to simulate the Zn-ligand (where ligand = S and N) interaction was non-bonded,[7] which entertains only electrostatic and van der Waals' forces.

After minimizing and subsequently equilibrating at 300 K the peptide, a production run of 10 ns was carried out in canonical ensemble, with a time step of 0.5 fs. In Fig. S4 we report the time series of the root mean square deviation (RMSD), the radius of gyration (R_g) and the average collision cross section calculated via the three above mentioned methods. The structure reference of the RMSD is the minimized consensus structure from the crystal structure as described in the main text, and here we consider RMSD from the backbone heavy atoms. It is evident that during the simulation the peptide conformation does not diverge much from the initial structure (the RSMD is always less than 4 °A). The Rg is calculated for all the atoms and testifies that the dimension of the peptide is roughly the same, except for a slight collapse at 8 ns. At or around this point, hydrophilic (charged) side chains form salt bridges between themselves and with charged atoms of the backbone.[8]

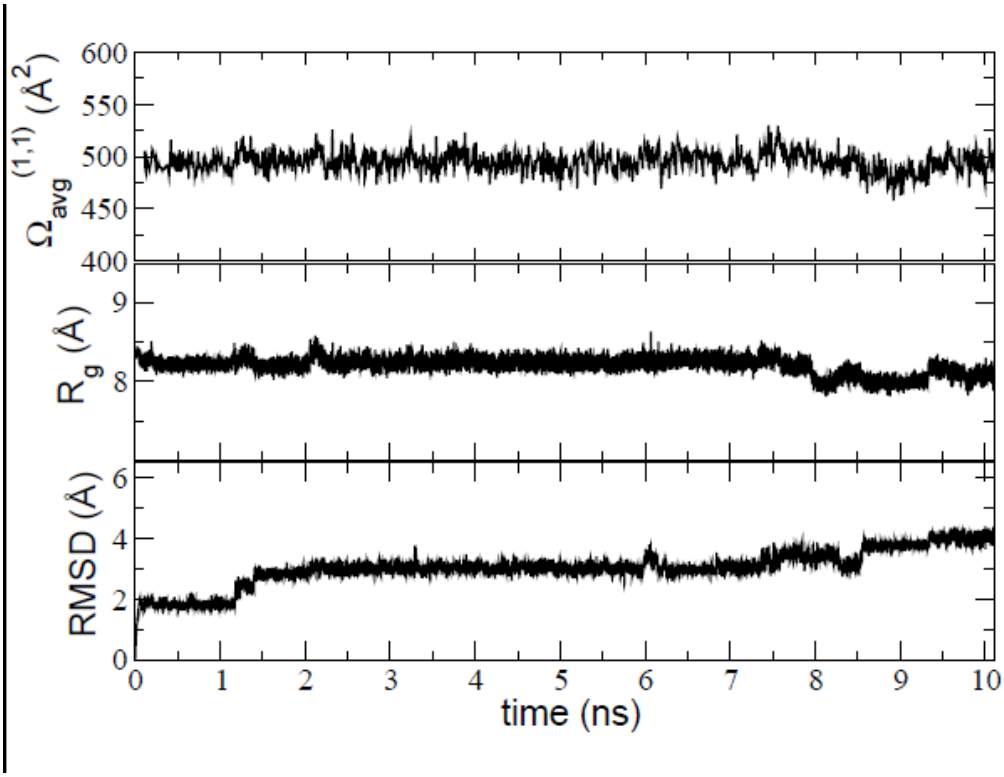

Figure S4- Holo-vCP1 time series of the average TM collision cross section (upper graph), radius of gyration (middle graph) and root mean square deviation (lower graph). Calculation of the 'all time' values was neglected for the heating process, (first 10 ps)

The trend of the calculated collision cross sections is the same for the three implemented methods; the absolute values reflect the expected deviations: PA method underestimated Ωavg by a 12%, EHS and TM are both near the experimental values.

The time averages of the cross sections are: 431 Å^2, 507 Å^{2}and 495 Å^2 for PA, EHS and TM respectively. Figure 4 shows a representative structure from this time course.

apo-vCP1

For the apo structure (Fig. 4) we used a protonation state found for pH = 7.00, which resulted in a total charge of +3.0 (as observed experimentally), with cysteines sulfur atoms are hydrogenated, in order to represent the fully reduced state of the system. We then followed two strategies:

1. We applied a simulated annealing (SA) protocol starting from a fully extended peptide. The protocol repeats n (=100) times an energy minimization, followed by "hot" dynamics at 800 K and subsequent stepwise cooling of the system until 0 K. For every minimized structure we calculated (via MOBCAL) the TM collision cross section, and the plot of its values versus energy values is given in Fig. S5. The average TM collision cross for these 100 structures Boltzmann weighted by their energy was 519 Å^2. To obtain a time evolution of the collision cross section MD simulations were performed on two representative structures as indicated in Figure S5: the first is the one with the lowest energy value and the second is the one whose TM collision cross section value is the nearest to that experimentally measured. These two structures were heated up to room temperature and then NVT dynamics up to 5 ns was followed, with a timestep of 0.5 fs. The time series of these two runs are given in Figs. S6 and S7 respectively. Their time averaged TM collision cross sections are 512 Å^{2}and 497 Å^2 respectively.

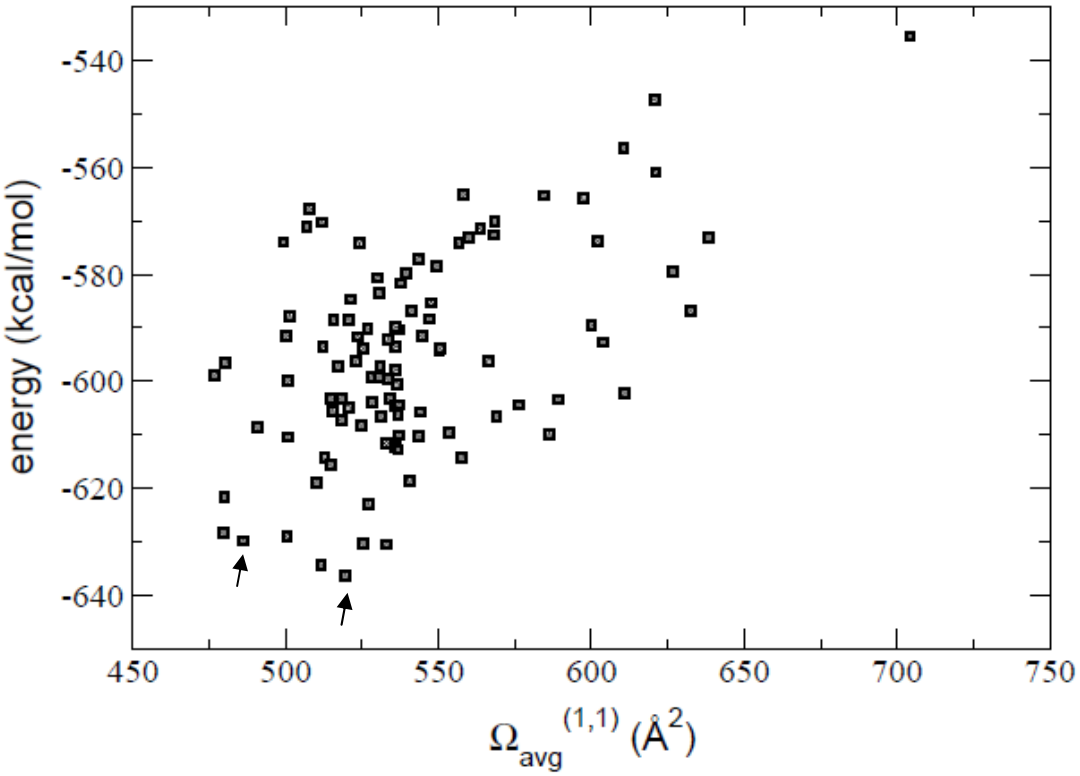

Figure S5 Scatter plot of the collision cross section (TM) versus energy for the 100 SA structures. Structures that were selected for subsequent MD are marked with arrows.

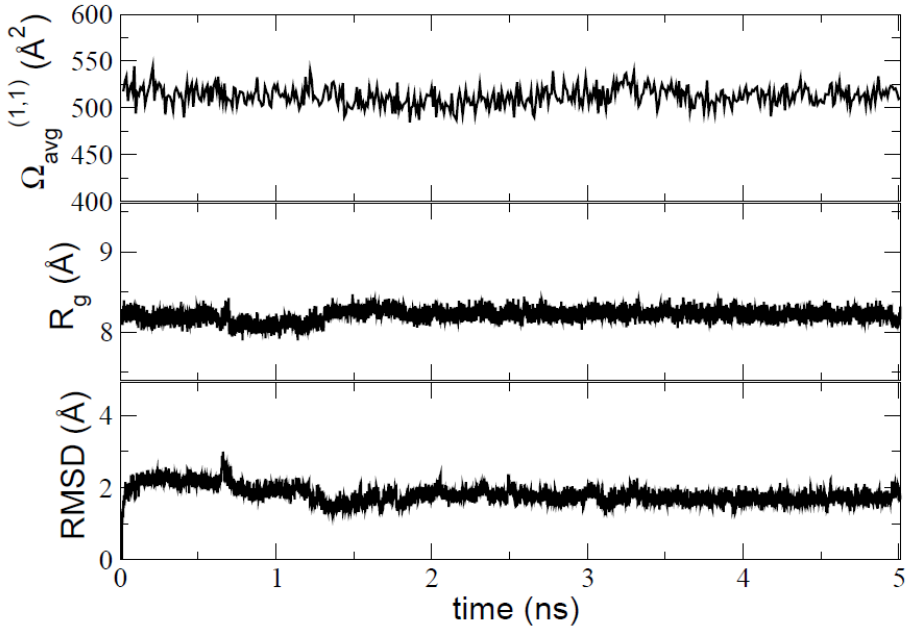

Figure S6: Time series for the apo-vCP1 structure with the lowest value of total energy among the 100 simulated annealing structures. Average TM collision cross section (upper graph), radius of gyration (middle graph) and root mean square deviation (lower graph). Calculation of the all time series was neglected for the heating process (first 10 ps).

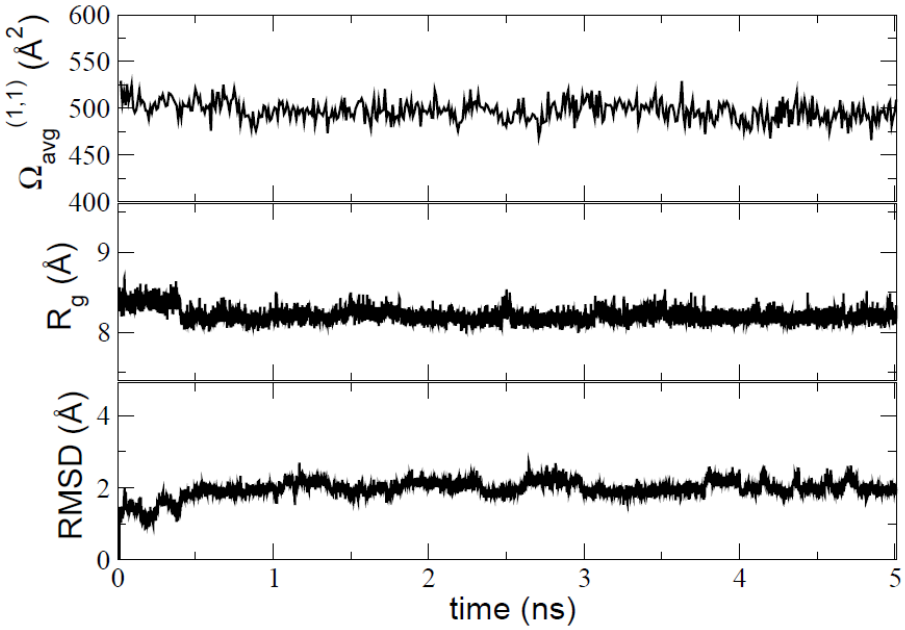

Figure S7: Time series for the apo-vCP1 simulated annealing structure with the CCS closest to the experimental one. Average TM CCS (upper graph), radius of gyration (middle graph) and root mean square deviation (lower graph). Calculation of the all time series was neglected for the heating process (First 10 ps).

2. In the second strategy the zinc atom was removed from the holo structure and an MD simulation run for to 10 ns. In Fig. S8 the related time series are shown and, in this case, the time averaged TM collision cross section is 501 Å^2. Whilst we think that strategy 1 is probably a better method by which to sample the gas phase conformations that we observe, to be consistent with the method taken for the holo peptide, Figure 4 (main text) contains a representative structure from strategy 2. The CCS's measured for conformations in each case are indistinguishable.

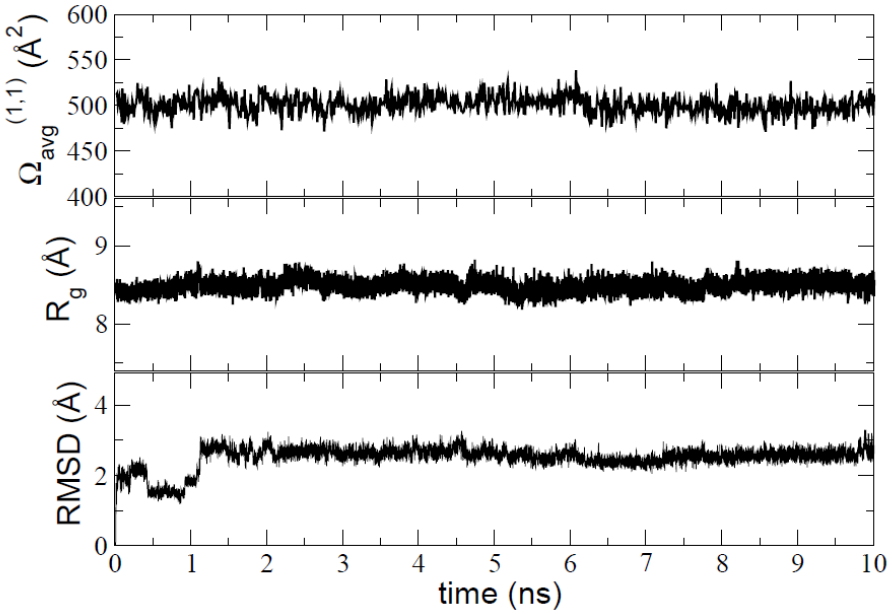

Figure S8: Time series for the apo-vCP1 system derived by direct removal of the zinc atom from the holo structure. Average TM CCS (upper graph), radius of yration (middle graph) and root mean square deviation (lower graph). Calculation of the all time series was neglected for the heating process (first 10 ps).

References

1. P. Dugourd, R. R. Hudgins, D. E. Clemmer and M. F. Jarrold, *Review of Scientific Instruments*, 1997, **68**, 1122-1129.
2. D. E. Clemmer and M. F. Jarrold, *Journal of Mass Spectrometry*, 1997, **32**, 577-592.
3. B. J. McCullough, J. Kalapothakis, H. Eastwood, P. Kemper, D. MacMillan, K. Taylor, J. Dorin and P. E. Barran, *Analytical Chemistry*, 2008, **80**, 6336-6344.
4. T. A. D. D.A. Case, T.E. Cheatham, III, C.L. Simmerling, J. Wang, R.E. Duke, R. Luo, R.C. Walker, W. Zhang, K.M. Merz, B.P. Roberts, B. Wang, S. Hayik, A. Roitberg, G. Seabra, I. Kolossváry, K.F. Wong, F. Paesani, J. Vanicek, X. Wu, S.R. Brozell, T. Steinbrecher, H. Gohlke, Q. Cai, X. Ye, J. Wang, M.-J. Hsieh, G. Cui, D.R. Roe, D.H. Mathews, M.G. Seetin, C. Sagui, V. Babin, T. Luchko, S. Gusarov, A. Kovalenko and P.A. Kollman . University of California, San Francisco, 2009.

5. A. A. Shvartsburg, G. C. Schatz and M. F. Jarrold, *J Chem Phys*, 1998, **108**, 2416-2423.
6. http://biophysics.cs.vt.edu/H++/.
7. D. V. Sakharov and C. Lim, *J Am Chem Soc*, 2005, **127**, 4921-4929.
8. K. Breuker and F. W. McLafferty, *P Natl Acad Sci USA*, 2008, **105**, 18145-18152.